Archives of Mechanics • Archiwum Mechaniki Stosowanej • 30, 4–5, pp. 619–627, Warszawa 1978

Hydrodynamic stability of cylindrical Couette-flow

K. G. ROESNER (KARLSRUHE)

THE STABILITY of the Couette-flow in the gap of finite width between two concentric, vertical cylinders is investigated numerically on the base of a linear stability analysis assuming that both the cylinders have different temperatures. The influence of gravitational effects on the stability behaviour of the laminar basic flow is studied and the computational results — obtained by two different numerical methods — are compared.

Stateczność przepływu typu Couette w szczelinie o skończonej szerokości między dwoma koncentrycznymi pionowymi walcami zbadano numerycznie. Wykorzystując analizę liniowej stateczności założono, że obydwa cylindry mają różne temperatury. Zbadano wpływ efektów grawitacyjnych na zachowanie się stateczności laminarnego podstawowego przepływu i porównano wyniki obliczeniowe uzyskane dwoma różnymi metodami numerycznymi.

Устойчивость течения типа Куэтта в щеии конечной ширины между двумя концентрическими вертикальными цилиндрами исследована численно. Используя анализ линейной устойчивости, предположено, что оба цилиндра имеют разные температуры. Исследовано вииянние гравитационных эффектов на поведение устойчивости ламинарного основного течения и сравнены расчетные результаты полученные двумя разными численными методами.

1. Introduction

EXPERIMENTAL investigations carried out by SNYDER and KARLSSON [1] describe the effect of a radial thermal gradient on the stability behaviour of the cylindrical Couette-flow. The results show for the case where the inner cylinder is rotating while the outer is at rest, that a small radial temperature gradient stabilizes the basic flow. Defining the Grashof-number on the base of the corresponding temperature difference, the interval of stabilization is given by $\mathrm{Gr} \leqslant 50$; $\mathrm{Gr}: = g\bar{\alpha}(\Delta R)^3 \delta T/\nu^2$; g = gravitational acceleration, α = = thermal expansion coefficient, ΔR = gap width between the cylinders, δT = temperature difference between outer and inner cylinder, ν = kinematic viscosity. When the Taylor-number $\mathrm{Ta}: = (R_1 \Omega_1 \Delta R/\nu)^2$; R_1 = radius of inner cylinder, Ω_1 = angular velocity of inner cylinder, is raised above the critical value, a toroidal secondary flow, the well-known Taylor-Görtler vortices, is observed. The critical Ta-number was in any case higher for small temperature differences than the value given by Taylor regardless whether the temperature of the inner cylinder was higher than the outer one or vice versa.

From the mathematical point of view the question arises whether the linear stability theory leads to the same results described above. As the temperature differences are small, in the calculations the influence of a variable kinematic viscosity is neglected. Only the presence of a convective flow in axial direction is taken into account on the base of the Boussinesq-approximation. For the numerical analysis two different methods were used. The first method was described in [3] and goes back to HARRIS and REID [4]. It will be

http://rcin.org.pl

"the method of linear combination" because the resulting eigenvalue problem is found by a linear combination of different solutions of a system of ordinary differential equations to fulfil the homogeneous boundary conditions at the ends of the interval.

The second method is based on the method of invariant imbedding. Details of the procedure are given in [5] and similar investigations can be found in the paper of WILKS and SLOAN [6].

2. The system of equation

The following set of equations is used to describe the flow of an incompressible viscous fluid in the finite gap between two coaxially rotating cylinders with a small radial temperature gradient. A cylindrical coordinate system is used:

Navier-Stokes equations:

(2.1)
$$\varrho_0\left(\frac{\partial v_r}{\partial t}+(\mathbf{v}\cdot\nabla)v_r-\frac{v_\varphi^2}{r}\right) = -\frac{\partial p}{\partial r}+\mu\left(\nabla^2 v_r-\frac{2}{r^2}\frac{\partial v_\varphi}{\partial \varphi}-\frac{v_r}{r^2}\right),$$
$$\varrho_0\left(\frac{\partial v_\varphi}{\partial t}+\mathbf{v}\cdot\nabla)v_\varphi+\frac{v_r v_\varphi}{r}\right) = -\frac{1}{r}\frac{\partial p}{\partial \varphi}+\mu\left(\nabla^2 v_\varphi+\frac{2}{r^2}\frac{\partial v_r}{\partial \varphi}-\frac{v_\varphi}{r^2}\right),$$
$$\varrho_0\left(\frac{\partial v_z}{\partial t}+(\mathbf{v}\cdot\nabla)v_z\right) = \varrho_0 g\bar{\alpha}(T-T_0)-\frac{\partial p}{\partial z}+\mu\nabla^2 v_z,$$
$$\mathbf{v}\cdot\nabla := v_r\frac{\partial}{\partial r}+\frac{v_\varphi}{r}\frac{\partial}{\partial \varphi}+v_r\frac{\partial}{\partial z},$$
$$\nabla^2 := \frac{\partial^2}{\partial r^2}+\frac{1}{r}\frac{\partial}{\partial r}+\frac{1}{r^2}\frac{\partial^2}{\partial \varphi^2}+\frac{\partial^2}{\partial z^2}.$$

Continuity equation:

(2.2)
$$\frac{\partial v_r}{\partial r}+\frac{v_r}{r}+\frac{1}{r}\frac{\partial v_\varphi}{\partial \varphi}+\frac{\partial v_z}{\partial z} = 0.$$

Energy equation:

(2.3)
$$\varrho_0 c\left(\frac{\partial T}{\partial t}+(\mathbf{v}\cdot\nabla)T\right) = \lambda\nabla^2 T.$$

ϱ_0 and T_0 are the density and temperature in the middle of the gap, v_r, v_φ, v_z are the radial, circumferential and axial velocity components related to a cylindrical coordinate system, p is the pressure, μ the viscosity of the fluid, c the specific heat, and λ the thermal conductivity.

As boundary conditions we assume that the inner cylinder is rotating with a fixed angular velocity while the outer cylinder is at rest. So the velocity at the inner boundary is given by

$$v_r = 0, \quad v_\varphi = R_1\Omega_1, \quad v_z = 0.$$

http://rcin.org.pl

At the outer boundary all velocity components vanish. We introduce dimensionless variables by relating any length to the gap width $\Delta R := R_2 - R_1$, the angular velocity to $R_1\Omega_1/\Delta R$, the temperature to the difference $\delta T := T_2 - T_1$ and the density to ϱ_0. It follows that the reference velocity is given by $R_1\,\Omega_1$, the time scale by $\Delta R/R_1\,\Omega_1$ and the pressure is related to $\varrho_0 R_1^2\Omega_1^2$.

The process of nondimensionalizing leads to three parameters: Taylor-number $\mathrm{Ta} := (\Delta R\cdot R_1\Omega_1/\nu)^2$, Grashof-number $\mathrm{Gr} := g\bar{\alpha}(\Delta R)^3\Delta T/\nu^2$, and Prandtl-number $\mathrm{Pr} := \nu/\varkappa$. The basic equations are now written in dimensionless form:

Navier-Stokes equations:

$$\frac{\partial v_r}{\partial t}+(\mathbf{v}\cdot\nabla)v_r+\frac{v_\varphi^2}{r} = -\frac{\partial p}{\partial r}+\frac{1}{\sqrt{\mathrm{Ta}}}\left(\nabla^2 v_r-\frac{2}{r^2}\frac{\partial v_\varphi}{\partial r}-\frac{v_r}{r^2}\right),$$

$$(2.1')\qquad \frac{\partial v_\varphi}{\partial t}+(\mathbf{v}\cdot\nabla)v_\varphi+\frac{v_r v_\varphi}{r} = -\frac{1}{r}\frac{\partial p}{\partial \varphi}+\frac{1}{\sqrt{\mathrm{Ta}}}\left(\nabla^2 v_\varphi+\frac{2}{r^2}\frac{\partial v_r}{\partial \varphi}-\frac{v_\varphi}{r^2}\right),$$

$$\frac{\partial v_z}{\partial t}+(\mathbf{v}\cdot\nabla)v_z = \frac{\mathrm{Gr}}{\mathrm{Ta}}(T-T_0)-\frac{\partial p}{\partial z}\frac{1}{\sqrt{\mathrm{Ta}}}\nabla^2 v_z.$$

Continuity equation:

$$(2.2')\qquad \frac{\partial v_r}{\partial r}+\frac{1}{r}\frac{\partial v_\varphi}{\partial \varphi}+\frac{v_r}{r}+\frac{\partial v_z}{\partial z} = 0.$$

Energy equation:

$$(2.3')\qquad \frac{\partial T}{\partial t}+(\mathbf{v}\cdot\nabla)T = \frac{1}{\mathrm{Pr}\sqrt{\mathrm{Ta}}}\nabla^2 T.$$

3. The basic solution

A linear stability analysis has to start from the exact solution of the set of equations (2.1') – (2.3'). An exact stationary solution for the case of a non-zero temperature gradient is given by the following formulas:

$$(3.1)\qquad v_\varphi^{(0)} = A^*r+\frac{B^*}{r},$$

$$(3.2)\qquad v_z^{(0)} = \frac{\mathrm{Gr}}{\sqrt{\mathrm{Ta}}}\left[\frac{C^*-D^*}{4}r^2+E^*\ln r+\frac{D^*}{4}r^2\ln r+F^*\right],$$

$$(3.3)\qquad T^{(0)} = T_1-\frac{\ln(r/R_1)}{\ln(R_1/R_2)},$$

$$(3.4)\qquad p^{(0)} = \frac{A^{*2}}{2}(r^2-R_1^2)-\frac{B^{*2}}{2}\left(\frac{1}{r^2}-\frac{1}{R_1^2}\right)+2A^*B^*\ln\frac{r}{R_1}.$$

http://rcin.org.pl

The constants $A^*, \ldots, F^*$ are defined in Appendix 1.

This basic solution differs from the well-known Couette-flow insofar as the axial velocity component $v_z^{(0)}$ does not vanish because of the existence of a convective flow induced by the radial temperature gradient. It should be emphasized that the basic streamlines have a helical character while the streamlines of the Couette-flow are circles.

4. Ansatz for the perturbations

For the formal investigation of the linear stability behaviour of the fluid motion we use an ansatz for all the unknown functions $v_r, v_\varphi, v_z, p, T$ in the following form:

$$f(r, \varphi, z; t) = f^{(0)}(r) + \varepsilon f^{(1)}(r, \varphi, z; t) + \ldots,$$

ε is the formal expansion parameter. After cancelling all nonlinear terms in the set of differential equations which arise from the ansatz above, we choose a special form of the disturbances allowed. Introducing an axial wave number $\alpha \in \mathrm{R}$ a circumferential wave number $\gamma \in \mathrm{Z}$, and an amplification factor $\beta \in \mathrm{C}$ the special type of disturbances is defined as follows:

$$f^{(1)} := f(r) \exp\{-i(\alpha z + \gamma\varphi + \beta t)\}. \tag{4.1}$$

If this ansatz is introduced into the system of partial differential equations for $v_r^{(1)}, v_\varphi^{(1)}, v_z^{(1)}, p^{(1)}, T^{(1)}$ it leads to a system of ordinary differential equations of the second order for the complex amplitudes $v_r(r), v_\varphi(r), v_z(r), p(r), T(r)$. Using the abbreviations $D := d/dr$; $D_* := d/dr + 1/r$ the system of ordinary differential equations can be given as

$$(D_* D + A_1)u + A_2 v + A_3 Dp + B_1 u = 0, \tag{4.2}$$

$$(D_* D + A_4)v + A_5 u + B_2 v + B_3 u + B_4 p = 0, \tag{4.3}$$

$$(D_* D + A_6)w + A_7 p + B_5 w + B_6 v + B_7 T = 0, \tag{4.4}$$

$$D_* u + A_8 w + B_8 v = 0, \tag{4.5}$$

$$(D_* D + B_9)T + B_{10} T = 0. \tag{4.6}$$

All terms containing the coefficients $B_1, \ldots, B_{10}$ are due to the temperature gradient. The coefficients $A_1, \ldots, A_8$ belong to the normal Couette-flow problem which leads to the well-known Taylor-Görtler vortices when no thermal effects are present.

The coefficients $A_i, i = 1, \ldots 8; B_j; j = 1, \ldots, 10$ are listed in Appendix 2 and 3.

5. The numerical calculation

The eigenvalue problem which is defined by the system (4.2) – (4.6) with homogeneous boundary conditions at both ends of the interval of integration is solved numerically by two different methods. The first methods starts with rewriting the system (4.2) – (4.6) into a system of first order. Starting with homogeneous boundary conditions for the unknown functions at the inner boundary the whole system of equations is solved for a sufficiently large number of initial conditions which differ only in the values for the derivatives of the

http://rcin.org.pl

unknown functions. To fulfil the zero boundary condition at the outer boundary, a suitable linear combination of the whole number of solutions is sought which leads to the so-called secular equation combining all the parameters of the problem

$$F(\alpha, \beta, \gamma, \mathrm{Gr}, \mathrm{Ta}, \mathrm{Pr}) = 0.$$

This method was already used by HARRIS and REID [4]. In the calculation the Pr-number was kept constant. Searching for neutral stability curves and secondary flows of toroidal character (= Taylor-Görtler vortices) we set $\beta = 0$, $\gamma = 0$, $\mathrm{Pr} = 6.25$. Then the triple $\alpha, \mathrm{Gr}, \mathrm{Ta}$ must be determined such that the secular equation is fulfilled.

For the integration of the set of first order equations the stiffness had to be proved. It could be shown that the system does not have a typical stiff character which means that the imaginary parts of the eigenvalues of the Jacobian matrix do not differ too much. For the solution the program EPISODE of HINDMARSH and BYRNE [7] was used which includes also the solution of stiff systems.

Using the invariant imbedding method, a Riccati transformation was applied which results in a nonlinear system of 64 real differential equations. The parameter sets which define the eigenvalues of the neutral stability curve are determined from the zeros of a de-

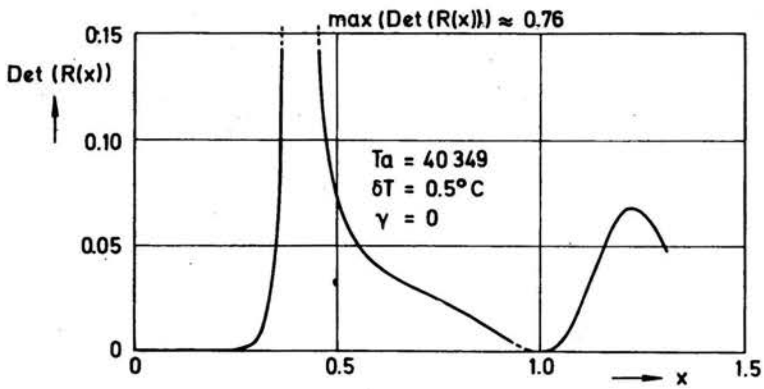

FIG. 1. Zero of $R(x)$ at $x = 1.0$ ($\gamma = 0$).

terminant. A typical behaviour of the determinant $R(x)$ along the variable x is shown in Fig. 1. For a toroidal secondary flow ($\gamma = 0$) a zero is found at $x = 1$ which defines the eigenvalue $\mathrm{Ta} := 40349$ for the temperature difference $\delta T = 0.5°\mathrm{C}$.

6. Comparison of computational results

For different values of δT the neutral stability curves were computed using both methods mentioned above. In a (α, Ta)-diagram (Fig. 2) the results of the method of linear combination are given by the broken lines. The full lines correspond to the invariant imbedding technique. Both sets of curves have in common that the critical Ta-number is raised when the temperature difference is raised. The curves for one value of δT do not coincide. The reason for it can be found in the inaccuracy of the invariant imbedding method which

http://rcin.org.pl

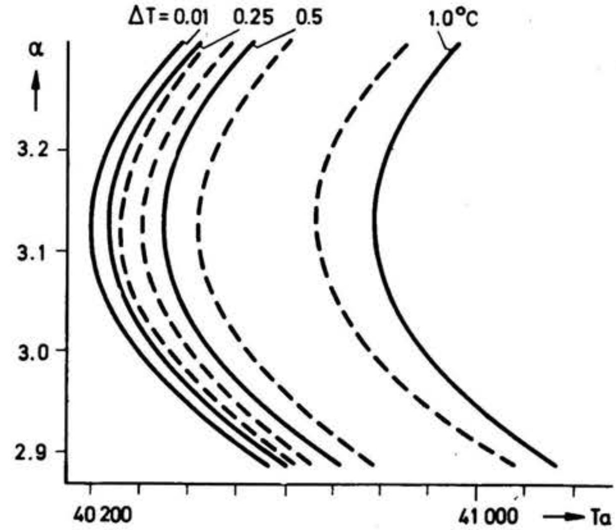

FIG. 2. Neutral stability curves for different temperature differences ($\Delta T = 0.01$, 0.025, 0.05, 1.0).

leads to a bigger amount of algebraic operations (e.g. matrix inversion and larger system of equations) compared to the method of linear combination. The maximal difference between critical Ta-numbers is given for $\delta T = 1°C$ by 0.2‰. This agreement of both computational results is satisfactory. When plotting the critical Ta-number versus the Gr-number

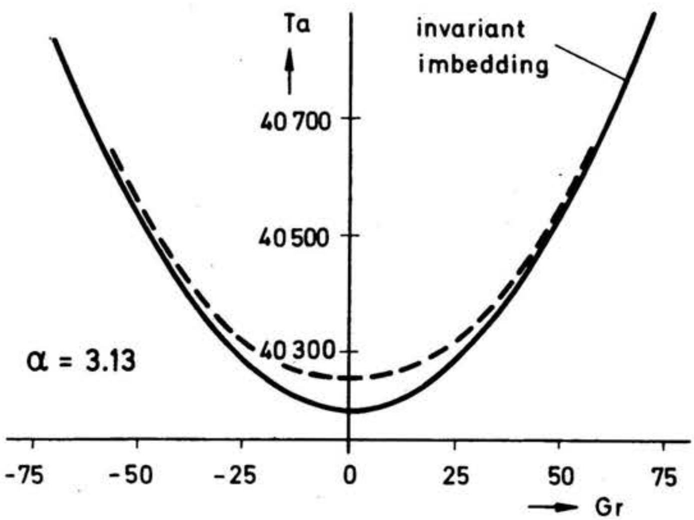

FIG. 3. Critical Ta-number versus Gr-number for small temperature differences.

the computational results give the two curves in Fig. 3. The broken line again corresponds to the method of linear combination while the full line is plotted from the invariant imbedding calculations. Both curves show in the vicinity of Gr = 0 that a small tempera-

http://rcin.org.pl

ture gradient leads to an increase of the Ta-number. This means that small temperature gradients in a cylindrical gap of two vertical cylinder have a stabilizing effect on the onset of a toroidal secondary flow.

7. Concluding remarks

An attempt was made to extend the calculations into a region of larger Gr-numbers beyond 50 to get the critical values of the Ta-number for the onset of the spiral secondary flow. The results on the base of the linear stability analysis do not show a significant changing of the character of the curves given in Fig. 3. Searching for zeros of $R(x)$ for the case of $\gamma \neq 0$ leads to results shown in Fig 4. No zero of $R(x)$ exists near the point $x = 1$.

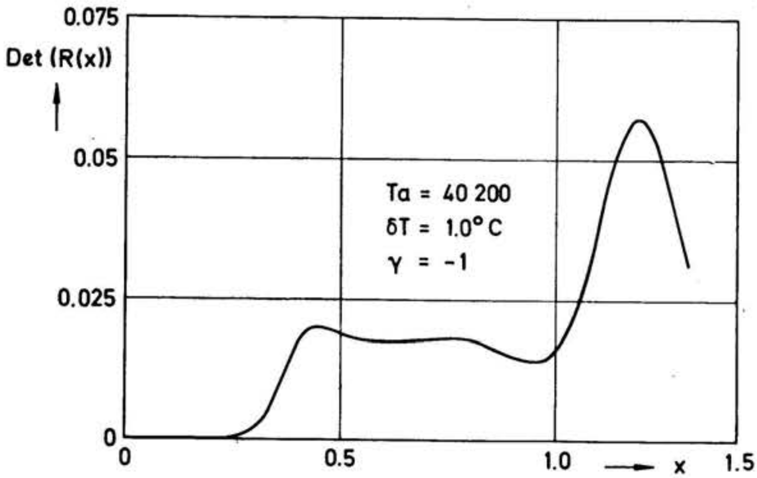

FIG. 4. Values of $R(x)$ along x for $\gamma = -1$.

On the base of a linear stability analysis with the assumption of small temperature gradients, it is only in the narrow vicinity of $\mathrm{Gr} = 0$ that reliable results can be observed which correspond to the experimental data by SNYDER and KARLSSON [1].

Appendix 1

$$A^*: = \frac{R_1 - R_2^2 \Omega_2}{R_1^2 - R_2^2},$$

$$B^*: = \frac{R_1 R_2^2 (1 - R_1 \Omega_2)}{R_2^2 - R_1^2},$$

$$C^*: = -\frac{\ln R_0}{\ln (R/R_2)}, \qquad R_0: = \frac{R_1 + R_2}{2},$$

$$D^*: = \frac{1}{\ln (R_1/R_2)},$$

http://rcin.org.pl

$$E^*:=\frac{(C^*-D^*)(R_1^2-R_2^2)+D^*(R_1^2\ln R_1-R_2^2\ln R_2)}{4\ln(R_2/R_1)},$$

$$F^*:=\frac{D^*-C^*}{4}R_1^2-\left(\frac{D^*}{4}R_1^2+E^*\right)\ln R_1.$$

Appendix 2

k	The coefficients A_k
A_1	$-\sqrt{\mathrm{Ta}}\,\beta_i-\frac{1}{r^2}-\alpha^2+i\sqrt{\mathrm{Ta}}\,\beta_r$
A_2	$2\sqrt{\mathrm{Ta}}\,\frac{v_\varphi^{(0)}}{r}$
A_3	$-\sqrt{\mathrm{Ta}}$
A_4	$-\sqrt{\mathrm{Ta}}\,\beta_i-\frac{1}{r^2}-\alpha^2+i\sqrt{\mathrm{Ta}}\,\beta_r$
A_5	$-\sqrt{\mathrm{Ta}}\left(\frac{dv_\varphi^{(0)}}{dr}+\frac{v_\varphi^{(0)}}{r}\right)$
A_6	$-\sqrt{\mathrm{Ta}}\,\beta_i-\alpha^2+i\sqrt{\mathrm{Ta}}\,\beta_r$
A_7	$i\alpha\sqrt{\mathrm{Ta}}$
A_8	$-i\alpha$

Appendix 3

k	The coefficients B_k
B_1	$-\frac{\gamma^2}{r^2}+i\sqrt{\mathrm{Ta}}\left(\alpha v_z^{(0)}+\gamma\frac{v_\varphi^{(0)}}{r}\right)$
B_2	$-\frac{\gamma^2}{r^2}+i\sqrt{\mathrm{Ta}}\left(\alpha v_z^{(0)}+\gamma\frac{v_\varphi^{(0)}}{r}\right)$
B_3	$-2i\frac{\gamma}{r^2}$
B_4	$+i\gamma\frac{\sqrt{\mathrm{Ta}}}{r}$

http://rcin.org.pl

k	The coefficients B_k
B_5	$-\dfrac{\gamma^2}{r^2}+i\sqrt{\mathrm{Ta}}\left(\alpha v_z^{(0)}+\gamma\dfrac{v_\varphi^{(0)}}{r}\right)$
B_6	$-\sqrt{\mathrm{Ta}}\dfrac{dv_z^{(0)}}{dr}$
B_7	$\dfrac{\mathrm{Gr}}{\sqrt{\mathrm{Ta}}}$
B_8	$-i\dfrac{\gamma}{r}$
B_9	$-\mathrm{Pr}\sqrt{\mathrm{Ta}}\beta_i-\dfrac{\gamma^2}{r^2}-\alpha^2+i\,\mathrm{Pr}\sqrt{\mathrm{Ta}}\left(\beta_r+\alpha v_z^{(0)}-\gamma\dfrac{v_\varphi^{(0)}}{r}\right)$
B_{10}	$-\mathrm{Pr}\sqrt{\mathrm{Ta}}\dfrac{dT^{(0)}}{dr}.$

References

1. H. A. SNYDER, S. K. F. KARLSSON, *Experiments on the stability of Couette motion with a radial thermal gradient*, Phys. Fluids, **7**, 10, 1696–1706, 1964.
2. G. I. TAYLOR, *Stability of a viscous liquid contained between two rotating cylinders*, Phil. Trans. Roy. Soc., A. **223**, 289–343, 1923.
3. K. G. ROESNER, *Fluid flow in a cylindrical gap with thermal gradient*, Proc. 2nd Workshop on Gases in Strong Rotation, April 6–8, Cadarache 1977.
4. D. L. HARRIS, W. H. REID, *On the stability of viscous flow between rotating cylinders*, J. Fluid Mech., **20**, Part 1, 95–101, 1964.
5. J. HEINRICHS, *Behandlung von Eigenwertproblemen mittels Invariant Imbedding*, Diplomarbeit, Math. Fak. der Albert-Ludwigs-Universität Freiburg, 1977 [unpublished].
6. G. WILKS, D. M. SLOAN, *Invariant imbedding, Riccati transformations and eigenvalue problems*, J. Inst. Maths. Applics, 18, 99–116, 1976.
7. G. D. BYRNE, A. C. HINDMARSH, *A polyalgorithm for the numerical solution of ordinary differential equations*, Prentice-Hall, New York 1971.

INSTITUT FÜR STRÖMUNGSLEHRE UND STRÖMUNGSMASCHINEN
UNIVERSITÄT KARLSRUHE.

Received October 15, 1977.

http://rcin.org.pl